Vol 459|18 June 2009|doi:10.1038/nature08052

LETTERS

Colorado Plateau magmatism and uplift by warming of heterogeneous lithosphere

Mousumi Roy[1], Thomas H. Jordan[2] & Joel Pederson[3]

The forces that drove rock uplift of the low-relief, high-elevation, tectonically stable Colorado Plateau are the subject of long-standing debate[1–5]. While the adjacent Basin and Range province and Rio Grande rift province underwent Cenozoic shortening followed by extension[6], the plateau experienced ~2 km of rock uplift[7] without significant internal deformation[2–4]. Here we propose that warming of the thicker, more iron-depleted Colorado Plateau lithosphere[8–10] over 35–40 Myr following mid-Cenozoic removal of the Farallon plate from beneath North America[11,12] is the primary mechanism driving rock uplift. In our model, conductive re-equilibration not only explains the rock uplift of the plateau, but also provides a robust geodynamic interpretation of observed contrasts between the Colorado Plateau margins and the plateau interior. In particular, the model matches the encroachment of Cenozoic magmatism from the margins towards the plateau interior at rates of 3–6 km Myr^{-1} and is consistent with lower seismic velocities[13] and more negative Bouguer gravity[14] at the margins than in the plateau interior. We suggest that warming of heterogeneous lithosphere is a powerful mechanism for driving epeirogenic rock uplift of the Colorado Plateau and may be of general importance in plate-interior settings.

Rock and surface uplift in high-elevation, plate-interior regions, such as the Ordos block of the North China craton or the Colorado Plateau in the western United States, are difficult to ascribe to plate-boundary deformation processes. These regions generally lack deformation[2–4,15] and are underlain by depleted lithosphere[8–10,15], and the relationship between their surface and/or rock uplift and plate-tectonic forces is unclear.

Previous ideas for Colorado Plateau rock and/or surface uplift fall into four categories: early- to mid-Cenozoic Laramide-orogeny-related shortening[2,4,5]; mid- to late-Cenozoic epeirogeny[3]; stream incision[1,16,17] and isostatic responses[7]; and dynamic uplift[18]. Here we show that even if the contributions from minor Laramide deformation[4] and flexural isostatic responses to extension at the plateau margins and to net Cenozoic erosion are removed, there is >1.6 km of residual rock uplift that must be explained by post-Laramide tectonic processes. Dynamic uplift mechanisms can drive only 400–500 m of this residual amount[18], leaving ~1.2 km of unexplained rock uplift. We propose thermal perturbation and re-equilibration as a general mechanism for driving rock uplift within plate interiors, particularly in regions of thicker, more depleted lithosphere adjacent to zones of extension, such as the Colorado Plateau. Our model differs from previous ideas of thermal modification of the Colorado Plateau[3] in that it relies on a post-Laramide process that is triggered by the removal of the Farallon slab and the onset of thinning in the Basin and Range and Rio Grande rift provinces. We show that thermal perturbation following mid-Tertiary removal of the Farallon slab can account for the majority of the observed rock uplift of the Colorado Plateau and, additionally, that this mechanism explains the observed rates of encroachment of the onset of Cenozoic magmatism onto the plateau.

The widespread distribution of shallow-marine and coastal-affinity sediments of late-Cretaceous age on the Colorado Plateau suggests relatively uniform elevation of the region at or near sea-level at that time. The present-day elevations of these strata can be reconstructed (including eustasy) to determine spatially varying net rock uplift and erosion functions across the plateau[7], with a mean of ~1.9 km net Cenozoic rock uplift (Fig. 1a) and net Cenozoic erosion of ~481 m (Fig. 1b). These reflect net deposition in early-Cenozoic time, mid-Cenozoic stability and then enhanced erosion since drainage integration in mid- to late-Cenozoic time[7].

Here we isolate the rock uplift of the Colorado Plateau that cannot be explained by Laramide crustal thickening, net Cenozoic erosion or flexural effects of extension in adjacent regions, and then model this residual rock uplift as being driven by thermal buoyancy modification. To remove contributions to the Cenozoic rock uplift of the Colorado Plateau from short-wavelength Laramide features (Fig. 1a), we smooth with a 2°-by-2° moving window (Fig. 1a, inset; Methods). In addition, we calculate the combined flexural response to spatially variable Cenozoic erosion (Fig. 1b) on the plateau and extension in adjacent regions (Methods). For reasonable flexural rigidities estimated for the Colorado Plateau[19], combined erosional and extensional unloading can drive ~0.5–0.6 km of rock uplift at the centre of the plateau and ~1 km at the edges that have undergone greater erosion or extension (Fig. 1c). Subtracting this response to unloading (Fig. 1c) from the smoothed rock uplift function (Fig. 1a, inset), we find the residual rock uplift (Fig. 1d). The average residual rock uplift increases from ~1.6 km at the centre of the plateau to a maximum of ~1.9–2.0 km approaching the margins, and then decreases at the extended western and southeastern margins (Fig. 1d). This residual cannot be explained by Laramide shortening or Cenozoic erosion and extension, and we model it here using mid-Tertiary buoyancy modification.

During Cenozoic time, the Colorado Plateau underwent subdued late-Mesozoic/early-Cenozoic shortening and minor extension, and was relatively unscathed by the voluminous and widespread mid-Tertiary magmatism (the 'ignimbrite flare-up'; Fig. 2) that affected regions surrounding the plateau[11,12,20]. Central to the idea of thermally driven rock uplift is transient heating of regions with thick lithosphere that protrude into the asthenosphere. Our hypothesis is that the Colorado Plateau represents one such region, where the difference in Cenozoic lithospheric thickness between the plateau and its surroundings[21] may be due to a combination of inherent chemical heterogeneity within North America[8–10], thinning of the plate in regions surrounding the plateau due to Cenozoic extension[6,21] and/or lithospheric modification in the Basin and Range

[1]Department of Earth and Planetary Sciences, University of New Mexico, Albuquerque, New Mexico 87131, USA. [2]Department of Earth Sciences, University of Southern California, Los Angeles, California 90089, USA. [3]Department of Geology, Utah State University, Logan, Utah 84322, USA.

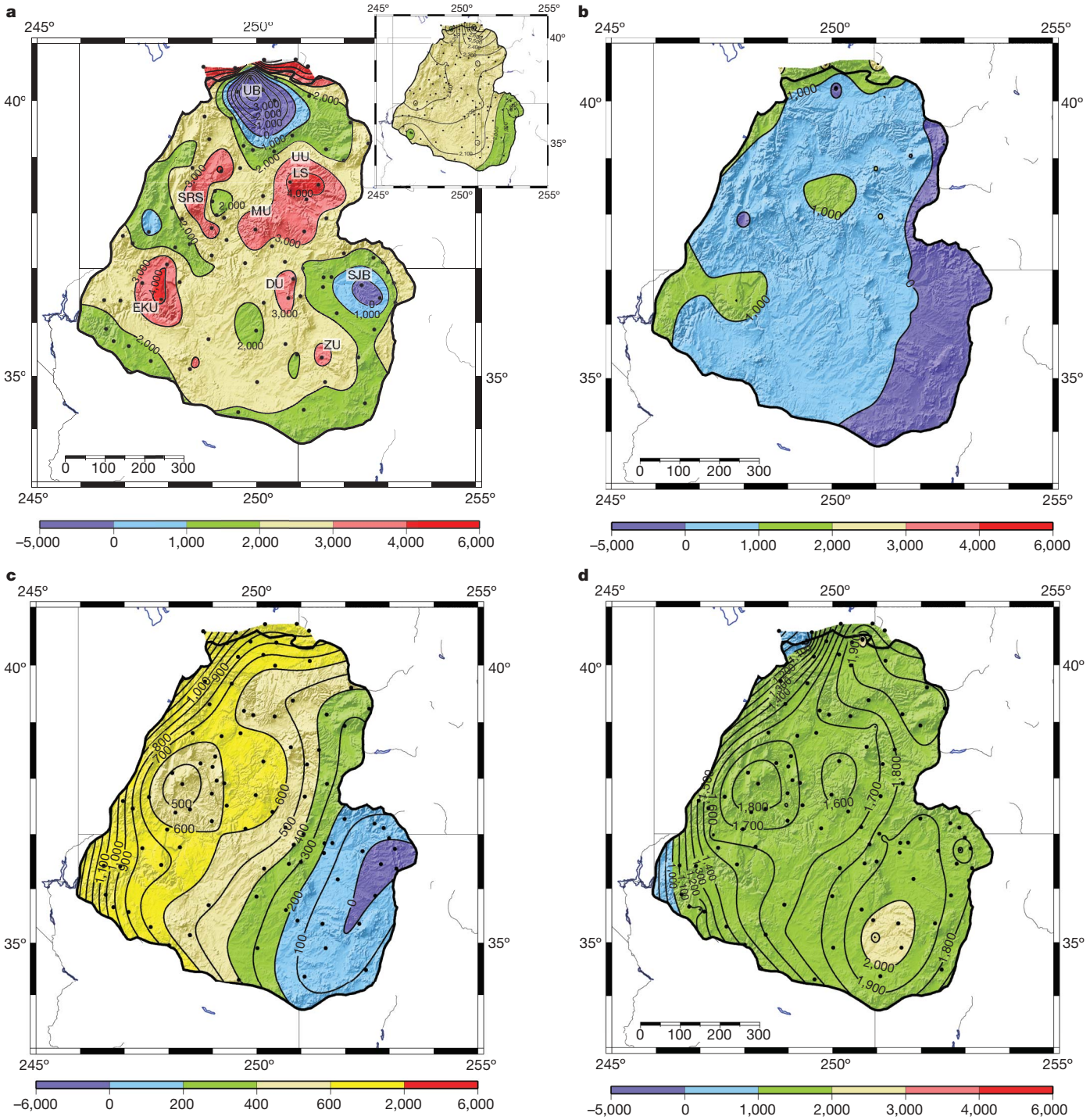

Figure 1 | Data (metres) used to derive the modelled residual rock uplift function. See Methods for details of model. **a**, Net Cenozoic (0–65 Myr ago) rock uplift across the Colorado Plateau[7], determined by stratigraphic constraints from field relations at the points marked (black dots). Laramide features: Uinta basin (UB), San Rafael swell (SRS), Uncompahgre uplift (UU), Monument uplift (MU), east Kaibab uplift (EKU), Defiance uplift (DU), San Juan basin (SJB), Zuni uplift (ZU), La Sal Mountains (LS). Inset, 2°-by-2° smoothed rock uplift function that effectively removes Laramide-related features. **b**, Net Cenozoic erosion function (smoothed rock uplift minus smoothed surface elevation; negative numbers denote burial). **c**, Flexural response to net Cenozoic erosion on the Colorado Plateau and extension in regions adjacent to the plateau (Methods), determined using a continuous plate with effective elastic plate thickness that was varied from $T_e = 20$ to 30 km (ref. 19). Representative results are shown for $T_e = 20$ km. **d**, Residual rock uplift function after flexural responses to erosion and extension (**c**) are removed from the smoothed rock uplift (inset in **a**). Scale bars in **a**, **b** and **d** show horizontal map distances in kilometres.

province upon removal of the Farallon slab roughly 30–40 Myr ago[11,12] (Fig. 3a).

Evidence for a chemically distinct Colorado Plateau lithosphere is seen in iron-depleted major-element compositions of mantle xenoliths from the western United States (Methods), suggesting that the plateau has undergone greater melt extraction than surrounding regions[8–10]. The enigmatic tectonic stability of the plateau maybe a result of this depletion[10], as the residuum following basalt removal is buoyant and/or of higher viscosity[22,23] and resists convective disruption[24] over timescales of 1 Gyr. Xenoliths also show that the Colorado Plateau may be in isopycnic equilibrium[10], with thicker lithosphere beneath the plateau than its surroundings. High seismic wave speeds

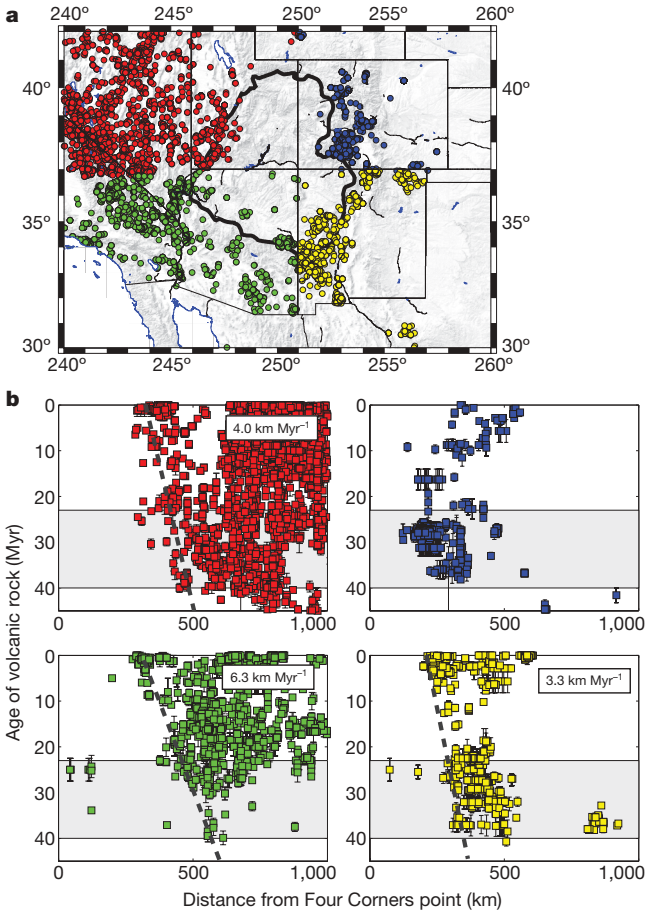

Figure 2 | Cenozoic magmatic patterns in the western United States, showing magmatic encroachment onto the Colorado Plateau. **a**, Distribution of Cenozoic volcanic rocks in the Western North American Volcanic and Intrusive Rock Database with age uncertainties of less than 5 Myr, colour-coded by azimuth relative to the 'Four Corners' point, where Colorado, New Mexico, Arizona and Utah meet. Locations do not include structural reconstruction (for example in highly extended regions), but this is not a great source of error in undeformed regions such as the Colorado Plateau (outlined). **b**, Igneous rock age as a function of distance from the Four Corners point, colour-coded by quadrant as in **a**. The dashed lines illustrate the encroachment of the onset of magmatism onto the plateau at the margins adjacent to Neogene extensional regions (northwest, southeast and southwest) at the rates indicated. The grey shading indicates the time of the late-Eocene/Oligocene ignimbrite flare-up, inferred to be the time of removal of the Farallon slab[11,12]. By restricting attention to volcanic rocks, we avoid including cooling ages of intrusions, but the rates of magmatic encroachment observed here are unchanged if all igneous rocks are used instead. Error bars indicate the minimum and maximum reported ages for a particular sample.

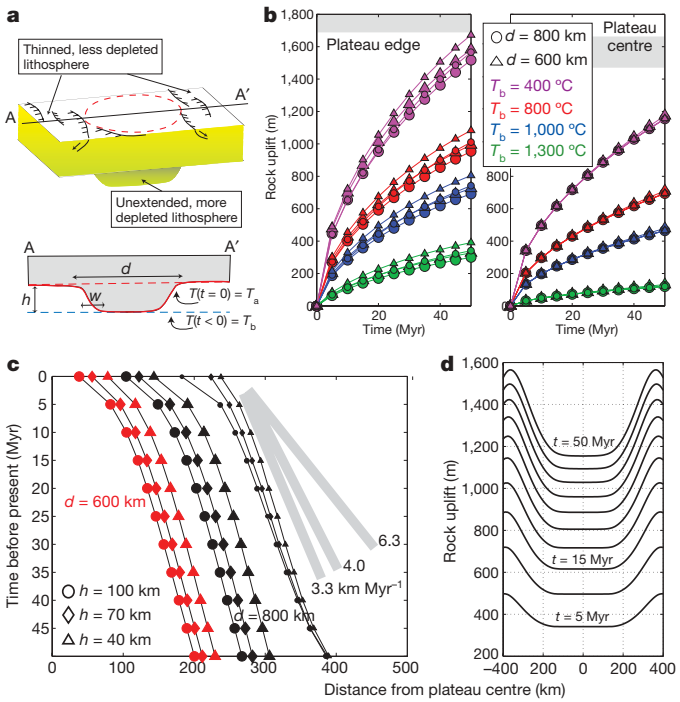

Figure 3 | Thermal and isostatic evolution during re-equilibration following a thermal perturbation at the base of a variable-thickness plate. **a**, Sketch of a heterogeneous plate, modelled as a cylindrically symmetric region that is thicker owing to a combination of greater depletion and lack of extension. **b**, Rock uplift at the edge and at the centre of the 'plateau' over 50 Myr of conductive relaxation for different values of d ($w = d/10$ and $h = 100$ km) and T_b, the initial basal temperature before mid-Tertiary time (modelled as $t = 0$), assumed to be the time of the thermal perturbation due to removal of the Farallon plate. The smaller symbols correspond to $T_e = 20$ km and the larger to $T_e = 30$ km (ref. 19). The observed range in residual rock uplift of the Colorado Plateau (Fig. 1d) is indicated by the grey regions. **c**, Lateral migration of the 1,200 °C isotherm at ~180-km depth as a function of d and h (results shown are for $T_b = 1{,}300$ °C). The slope of the lines represents the migration rate, which is a strong function of w, as illustrated by the lines with the smallest black symbols and fastest rate of encroachment: $d = 800$ km and $w = d/100$. All other results are shown for a larger value, $w = d/10$. Grey bars indicate rates observed in the migration of the onset of magmatism in Fig. 2b. **d**, Spatiotemporal pattern of rock uplift (every 5 Myr) for $d = 800$ km, $w = d/100$, $T_e = 30$ km and $T_b = 400$ °C, showing higher values at the margins than in the interior and migration of the point of highest uplift slightly in from the margins of the plateau.

exist beneath the plateau to depths of >100 km, whereas adjacent regions have slower wave speeds, suggesting thicker lithosphere beneath the plateau[12,13]. In the following, therefore, we assume that the Colorado Plateau lithosphere is thicker than its surroundings owing to a combination increased depletion of the plateau and thinning of adjacent regions, although we do not require the plateau to be isopycnic.

The Colorado Plateau is characterized by a lack of Cenozoic magmatism (Fig. 2a) and an encroachment of the onset of magmatism onto the plateau since mid-Tertiary time[25] (we define this encroachment as an enveloping surface on the space-time pattern of magmatism; Fig. 2b). The voluminous mid-Tertiary (23–40 Myr ago) ignimbrite flare-up accompanied the transition in deformation styles in the western United States from Mesozoic subduction to Neogene–present extension. It has been suggested that hydration of North America during Mesozoic subduction followed by the removal of the Farallon plate drove the voluminous magmatic response[11,12,20], and we assume that mid-Tertiary time coincided with the transition from cooler mantle-wedge conditions beneath the plate[26,27] to hotter conditions as hot asthenosphere contacted the base of the plate. We propose that transient heating of the thicker Colorado Plateau lithosphere was triggered by the mid-Tertiary thermal perturbation and was aided by the fact that regions surrounding the plateau experienced coeval plate thinning. In our models, the contrast in thermal boundary thickness between the Colorado Plateau and its surroundings evolves as the plateau warms, but we ignore time-dependent extension of surrounding regions.

We combine flexure with three-dimensional conductive models of heat transfer (Methods Summary) over a 40–50-Myr interval in an idealized variable-thickness plate representing the combined effects of greater depletion in the central part and extensional thinning of the surrounding, less depleted regions (Fig. 3a; Methods). The 50-Myr model time interval is chosen to encompass the time since the ignimbrite flare-up in the western United States (~25–40 Myr ago) and captures expected thermal effects in the Colorado Plateau following removal of the Farallon slab[11,12].

Our models indicate that transient warming since mid-Tertiary time (defined as $t = 0$) thins the thermal boundary layer and drives

rock uplift of the Colorado Plateau over the last 20–40 Myr (Fig. 3b), producing greater rock uplift at the margins than in the plateau interior, with the maximum rock uplift occurring just inside the plateau margins (Fig. 1d). Buoyancy modification is driven by the inward migration of a conductive heating front (represented, for example, by the lateral migration of the $T = 1{,}200\ ^{\circ}C$ isotherm measured at a depth of ~180 km) at a rate that is governed by the length scale, w, over which the plate thickness changes (Fig. 3a) and has a minor dependence on the excess thickness, h (Fig. 3c).

The expected amplitude of rock uplift from conductive heating depends on the initial thermal structure and the shape of the plate (Fig. 3b; Methods). For a diameter of $d = 800$ km, comparable to that of the Colorado Plateau, and an initial basal temperature of $T_b = 400\ ^{\circ}C$, we expect rock uplift of 1.2–1.4 km at the centre and 1.6–1.7 km at the edges in 30 Myr. This low initial basal temperature corresponds to a plate that is insulated by the presence of the Farallon slab (before thermal relaxation), consistent with xenolith palaeothermometry and thermal modelling of the Laramide orogeny[26,27]. Although shallow subduction of the Farallon plate has been inferred from thermal histories of rocks[26,27], we note that our models do not explicitly require it. Our models require a mid-Tertiary thermal perturbation at the base of the Colorado Plateau and surroundings, and our results lend support to the idea that removal of a shallowly subducting Farallon plate would provide such a thermal perturbation.

The predicted timing and spatial distribution of rock uplift may be tested using detailed studies of rock cooling and exhumation together with stratigraphic constraints[16,17]. We note that the southern margin of the plateau has experienced greater early-Cenozoic exhumation but little late-Cenozoic erosion outside the narrow Grand Canyon[7,17]. In contrast, the plateau interior has been affected by a pulse of late-Cenozoic incision along the trunk drainage system[7], decoupled from the timing of thermally driven rock uplift (Fig. 1b). A regionally extensive data set of long-term exhumation is required to elucidate this further and separate the progressive uplift predicted in our model (Fig. 3b) from the signal of more recent base-level fall along the drainage system, although periods of rapid exhumation are easier to detect in rock cooling data than are slow, protracted rock uplift and erosion.

Although we do not explicitly include partial melting in our model, if we use the $T = 1{,}200\ ^{\circ}C$ isotherm as a first-order proxy for the onset of hydrous melting in the upper mantle[28], the rates of inward migration of the heating front are predicted to be 3–6 km Myr^{-1} for a wide range of plateau diameters ($d = 600$–800 km, comparable to the width of the Colorado Plateau), consistent with the inferred rates at which the onset of magmatism encroaches onto the plateau (Figs 2 and 3c). We also observe a late-stage increase in this rate as vertically rising and inward-migrating conductive heating fronts pass a given point (change in slope between 0 and 5 Myr in Fig. 3c). Future, more detailed, comparisons with phase relationships in a melting model must incorporate variable chemistry and hydration of source regions[12] and changes in both chemical and thermal buoyancy during and following the mid-Tertiary ignimbrite flare-up[14].

The observed asymmetry in the rate of encroachment of the onset of Cenozoic magmatism onto the Colorado Plateau (4–6.3 km Myr^{-1} at the northwestern and southwestern margins adjacent to the highly extended Basin and Range province, versus 3.3 km Myr^{-1} at the southeastern margin adjacent to the significantly less extended Rio Grande rift province) is predicted by our model to be a consequence of variations in the excess thickness, h, of the plateau relative to its surroundings and the horizontal scale, w, over which plate thickness varies (w is predicted to be shorter at the margins adjacent to the Basin and Range province than at the margin adjacent to the Rio Grande rift province). Our models predict the upper mantle at the margins of the Colorado Plateau to be warmer and lower in density than the upper mantle in its interior, consistent with lower upper-mantle seismic velocities[12,13] and lower Bouguer gravity[14]. Additionally, the magmatic alteration of the margins of the plateau predicted by our thermal model is consistent with xenolith populations that at the margins of the plateau contain more metasomatized, pyroxenite-bearing rocks than they do in the interior[14]. In particular, the presence of garnet-websterite xenoliths hosted in 3-Myr-old volcanic fields at the margin of the Colorado Plateau[14] is consistent with metasomatic alteration[9,14,26] at the edges of the intact but altered plateau lithosphere. Finally, comparisons of inferred upper-mantle temperatures from seismic velocity and heat flow show evidence for a transient thermal regime in the plateau and the Rio Grande rift[29], at the margins of the plateau.

To conclude, the predicted pattern of thermally driven mid-Tertiary–present rock uplift of the Colorado Plateau, with smaller rock uplift in the interior than at the margins (Fig. 3b, d), is comparable to the patterns observed in the residual rock uplift of the plateau (Fig. 1d). Conductive re-equilibration explains a large fraction of the residual rock uplift, although to match the full magnitude of the rock uplift (particularly in the central plateau) and to match local highs and lows, models will probably need to include the effects of variable plate rigidity, spatially variable extension and dynamic uplift[18]. Additionally, part of the discrepancy between predicted and observed rock uplift may be due to non-zero average Laramide rock uplift. Our model nevertheless provides a coherent thermal process that explains disparate observations such as the pattern and rate of encroachment of the onset of Cenozoic magmatism from the margins to the plateau interior (Figs 2b and 3c), lower seismic velocities[12,13] at the margins than in the plateau interior and lower-density upper mantle at the margins than in the interior (as inferred from xenoliths and gravity[14]), and patterns of rock cooling across the southern plateau[17]. Thermal perturbation, re-equilibration and the accompanying magmatism in plate-interior settings is likely to be an important process for the rejuvenation and refertilization of cratonic regions and may drive significant intra-plate epeirogenic rock uplift.

METHODS SUMMARY

We calculate flexural isostatic responses by convolving the expected local response with the two-dimensional Green's function for an elastic plate of uniform rigidity[30]. We use two rigidities, corresponding to effective elastic plate thicknesses of $T_e = 20$ and 30 km, chosen to bracket the value of $T_e = 22$–25 km estimated from coherence of gravity and topography for the Colorado Plateau[19]. The response of the Colorado Plateau to extensional unloading at margins adjacent to the Basin and Range and Rio Grande rift provinces is calculated using published basin loads from joint inversions of gravity and topography (Methods).

We assume a linear initial geotherm with $T_0 = 0\ ^{\circ}C$ at the surface and a basal temperature of $T_b = 400$, 800, 1,000 or 1,300 °C (Fig. 3b). These T_b values represent normal to cooler-than-normal mantle-wedge conditions[26,27] before the removal of the Farallon slab at $t = 0$. Immediately after $t = 0$, the plate is subjected to a new basal temperature, $T_a = 1{,}300\ ^{\circ}C$ and allowed to re-equilibrate. We assume a thermal diffusivity of $\kappa = 1 \times 10^{-6}\ m^2\ s^{-1}$, zero upper-mantle heat production and uniform crustal heat production of $3 \times 10^{-6}\ W\ m^{-3}$ over a depth range of 0–15 km. Conduction drives lateral and basal heating of the thicker lithosphere, so initially warped isotherms flatten out. The assumption of uniform temperatures beneath the plate (ignoring the adiabatic gradient) is equivalent to the assumption that convection maintains contact between hot asthenosphere and the plate.

We use the time-dependent thermal structure to derive a time-dependent density (assuming a coefficient of thermal expansion of $\alpha = 2.5 \times 10^{-5}\ K^{-1}$) and transient flexural isostatic responses. The conductive timescale for the steady state is ~1 Gyr, but warming of the Colorado Plateau is enhanced by three-dimensional conduction inward from the margins of the ~600–800-km-diameter region. The conductive timescale, τ, scales with area ($\tau \approx (\text{area})^{1/2}/\kappa$) and our models show that for the typical diffusivity assumed, transient responses over ~10–100 Myr will be a significant fraction of the total steady-state response for regions of length scale 10^2 km.

Full Methods and any associated references are available in the online version of the paper at www.nature.com/nature.

Received 4 June 2008; accepted 6 April 2009.

1. Hunt, C. B. Cenozoic geology of the Colorado Plateau. *Prof. Pap. US Geol. Surv.* **279** (1956).

2. Bird, P. Continental delamination and the Colorado Plateau. *J. Geophys. Res.* **84,** 7561–7571 (1979).
3. Morgan, P. & Swanberg, C. A. On the Cenozoic uplift and tectonic stability of the Colorado Plateau. *J. Geodyn.* **3,** 39–63 (1985).
4. Spencer, J. E. Uplift of the Colorado Plateau due to lithospheric attenuation during Laramide low-angle subduction. *J. Geophys. Res.* **101,** 13595–13609 (1996).
5. McQuarrie, N. & Chase, C. G. Raising the Colorado Plateau. *Geology* **28,** 91–94 (2000).
6. Wernicke, B., Christiansen, R. L., England, P. C. & Sonder, L. J. Tectonomagmatic evolution of Cenozoic extension in the North American Cordillera. *Spec. Publ. Geol. Soc. (Lond.)* **28,** 203–221 (1987).
7. Pederson, J. L., Mackley, R. D. & Eddleman, J. L. Colorado Plateau uplift and erosion evaluated using GIS. *GSA Today* **12,** 4–10 (2002).
8. Alibert, C. Peridotite xenoliths from the western Grand Canyon and the Thumb: a probe into the subcontinental mantle of the Colorado Plateau. *J. Geophys. Res.* **99,** 21605–21620 (1990).
9. Smith, D. Insights into the evolution of the uppermost continental mantle from xenolith localities on and near the Colorado Plateau and regional comparisons. *J. Geophys. Res.* **105,** 16769–16781 (2000).
10. Lee, C.-T. *et al.* Preservation of ancient and fertile lithospheric mantle beneath the southwestern United States. *Nature* **411,** 69–73 (2001).
11. Humphreys, E. D. Post-Laramide removal of the Farallon slab, western United States. *Geology* **23,** 987–990 (1995).
12. Humphreys, E. D. *et al.* How Laramide-age hydration of North American lithosphere by the Farallon slab controlled subsequent activity in the western United States. *Int. Geol. Rev.* **45,** 575–595 (2003).
13. Sine, C. R. *et al.* Mantle structure beneath the western edge of the Colorado Plateau. *Geophys. Res. Lett.* **35,** doi:10.1029/2008GL033391 (2008).
14. Roy, M., MacCarthy, J. K. & Selverstone, J. Upper mantle structure beneath the eastern Colorado Plateau and Rio Grande rift revealed by Bouguer gravity, seismic velocities, and xenolith data. *Geochem. Geophys. Geosyst.* **6,** doi:10.1029/2005GC001008 (2005).
15. Menzies, M., Xu, Y., Zhang, H. & Fan, W. Integration of geology, geophysics and geochemistry: a key to understanding the North China Craton. *Lithos* **96,** 1–21 (2007).
16. McMillan, M. E., Heller, P. L. & Wing, S. L. History and causes of post-Laramide relief in the Rocky Mountain orogenic plateau. *Bull. Geol. Soc. Am.* **118,** 393–405 (2006).
17. Flowers, R., Wernicke, B. P. & Farley, K. A. Unroofing, incision and uplift history of the southwestern Colorado Plateau from (U-Th)/He apatite thermochronometry. *Bull. Geol. Soc. Am.* **120,** 571–587 (2008).
18. Moucha, R. *et al.* Mantle convection and the recent evolution of the Colorado Plateau and the Rio Grande Rift valley. *Geology* **36,** 439–442 (2008).
19. Lowry, A. & Smith, R. B. Flexural rigidity of the Basin and Range-Colorado Plateau-Rocky Mountain transition from coherence analysis of gravity and topography. *J. Geophys. Res.* **99,** 20123–20140 (1994).
20. Lipman, P. W. & Glazner, A. F. Introduction to middle Tertiary Cordilleran volcanism – Magma sources and relations to regional tectonics. *J. Geophys. Res.* **96,** 13193–13199 (1991).
21. Wang, K., Plank, T., Walker, J. D. & Smith, E. I. A melting profile across the Basin and Range, SW USA. *J. Geophys. Res.* **107,** doi:10.1029/2001JB000209 (2002).
22. Kelly, R. K., Kelemen, P. B. & Jull, M. Buoyancy of the continental upper mantle. *Geochem. Geophys. Geosyst.* **4,** doi:10.1029/2002GC000399 (2003).
23. Schutt, D. L. & Lesher, C. E. Effects of melt depletion on the density and seismic velocity of garnet and spinel lherzolite. *J. Geophys. Res.* **111,** doi:10.1029/2003JB002950 (2006).
24. Lenardic, A., Moresi, L.-N. & Mülhaus, H. Longevity and stability of cratonic lithosphere: insights from numerical simulations of coupled mantle convection and continental tectonics. *J. Geophys. Res.* **108,** doi:10.1029/2002JB001859 (2003).
25. Wenrich, K. J. *et al.* Spatial migration and compositional changes of Miocene-Quaternary magmatism in the western Grand Canyon. *J. Geophys. Res.* **100,** 10417–10440 (1995).
26. Smith, D. & Griffin, W. L. Garnetite xenoliths and mantle-water interactions below the Colorado Plateau, southwestern United States. *J. Petrol.* **46,** 1901–1924 (2005).
27. English, J. M., Johnston, S. T. & Wang, K. L. Thermal modeling of the Laramide orogeny: testing the flat-slab subduction hypothesis. *Earth Planet. Sci. Lett.* **214,** 619–632 (2003).
28. Katz, R. F., Spiegelman, M. & Langmuir, C. H. A new parametrization of hydrous melting. *Geochem. Geophys. Geosyst.* **4,** doi:10.1029/2002GC000433 (2003).
29. Goes, S. & van der Lee, S. Thermal structure of the North American uppermost mantle inferred from seismic tomography. *J. Geophys. Res.* **107,** doi:10.1029/2000JB000049 (2002).
30. Jones, C. H., Unruh, J. R. & Sonder, L. J. The role of gravitational potential energy in active deformation in the southwestern United States. *Nature* **381,** 37–41 (1996).

Supplementary Information is linked to the online version of the paper at www.nature.com/nature.

Acknowledgements This work was supported by the US National Science Foundation (NSF) grants EAR0538022 and EAR0408513 and an NSF Advance Fellowship from the Lamont-Doherty Earth Observatory to M.R. The authors thank C. Jones for comments that significantly improved the model and manuscript and C. Callahan for compiling a database of xenolith compositions. The ideas in this paper benefited from our discussions with M. Hirschmann, L. Farmer, J. Selverstone and K. Condie.

Author Contributions M.R. was responsible for all of the data analysis and model calculations, T.H.J. provided ideas on the implications of the chemical heterogeneity of the Colorado Plateau and J.P. provided estimates and interpretation of field-based rock uplift and erosion.

Author Information Reprints and permissions information is available at www.nature.com/reprints. Correspondence and requests for materials should be addressed to M.R. (mroy@unm.edu).

METHODS

Data analysis. The estimates of net Cenozoic rock uplift across the Colorado Plateau (Fig. 1a) are based on outcrops and reconstructions of the base of late-Cretaceous marine-affinity strata[7], including a eustatic correction for higher Cretaceous sea level (Supplementary Information). At the majority of locations where the base of the late-Cretaceous marine-affinity strata outcrops, uncertainties from estimating the present-day elevation of this stratigraphic datum are <1 m; at the minority of locations where the strata are reconstructed, uncertainties are larger, but are generally <100 m. Additional minor uncertainties (<1 m) arise from uncertainties in the 90-m digital elevation model used[7].

We note that Laramide features correspond to locally high rock uplift. To remove these short-wavelength features and focus on regional patterns, we smooth the rock uplift function with a moving-window average (the results are unchanged for windows ranging from 1° by 1° to 2° by 2°; Fig. 1a, inset). The northern margin of the plateau, which has not undergone extension (in contrast to the western, southern and eastern margins), has large positive rock uplift values (>5 km) in the unextended, Laramide-age Uinta Mountains; after smoothing, these off-plateau points lead to positive rock uplift numbers in the Uinta basin (Fig. 1a, inset). The smoothed net Cenozoic erosion function (Fig. 1b) is the difference between the smoothed net Cenozoic rock uplift and smoothed present-day surface elevation (the topography was smoothed by averaging using the same windows as the rock uplift function).

Flexural response of the Colorado Plateau to adjacent extension. The regions to the west, south and east of the plateau have undergone variable extension over the past 30 Myr, and the flexural response to this extension should affect rock uplift at the margins of the plateau. The flexural response at the margins of the highly extended Basin and Range province is difficult to estimate because of the wide, distributed nature of the deformation complicated by magmatic loads[6], whereas the more compact, relatively amagmatic basins of the Rio Grande rift allow joint analysis of gravity and topography to estimate basin loads[31]. Upward-directed basin loads estimated in the Rio Grande rift range from 3.5×10^{11} N m^{-1} (northern Albuquerque basin, 17–28% extension) to 1.6×10^{12} N m^{-1} (Tularosa basin, 40–50% extension)[31]. We use the higher value in our calculations of the flexural response to extension at the margins of the Colorado Plateau and assume that the load is imposed uniformly over all regions outside the plateau. The flexural response to this load within the plateau (Supplementary Fig. 1) is then added to the flexural response to net Cenozoic erosion[7], and this sum is subtracted from the smoothed rock uplift function (Fig. 1a, inset).

The extensional loads assumed here are idealized, and we acknowledge that extension surrounding the plateau is spatially variable. This model provides a first-order estimate of the effects of extension surrounding the western, southern and eastern margins of the plateau. However, the northern and northeastern margins are not extended, so the calculated flexure is not relevant in this area and we caution that the resulting inferred residual rock uplift in the Uinta basin (Fig. 1d) is probably an underestimate. By assuming that large-magnitude extension uniformly surrounds the Colorado Plateau, however, we obtain a maximum estimate for rock uplift due to spatially variable extension adjacent to the plateau. This is an appropriate first-order approach because we wish to determine the minimum residual rock uplift that is unexplained by processes such as erosion and extension. Our assumption of a uniform-rigidity plate is likely to be invalid at the margins of the extensional zones adjacent to the plateau, which are probably of lower rigidity[19,31] (alternatively, the plate may not be continuous), so the residual rock uplift magnitude is probably an overestimate. In this work, we consider the effects of net Cenozoic erosion (Fig. 1b) and net Cenozoic extension (Supplementary Fig. 1), ignoring any temporal variations in the onset and duration of extension adjacent to the Colorado Plateau.

Magnesium number of on- and off-plateau xenoliths. We use published xenolith compositions[8–10,32–56] and divide the rocks into on- and off-plateau groups (Supplementary Fig. 2). Xenoliths on the plateau are distinctly more magnesian than those off the plateau, both for whole-rock[32–40] and olivine[8,32–56] analyses (Supplementary Fig. 2).

Thermal model. In our model, the initial thermal state corresponds to flat isotherms ($t<0$; Fig. 3a), but at $t=0$ we impose a thermal perturbation such that the base of the variable-thickness plate is an isotherm at $T_a = 1{,}300$ °C. The thicker plate in the Colorado Plateau is assumed to reflect a combination of greater depletion and a lack of Cenozoic extension compared with the surroundings. We solve the heat equation for $t>0$ within the variable-thickness thermal boundary layer by assuming that the surface and basal temperatures are fixed, at $T_0 = 0$ °C and $T_a = 1{,}300$ °C, respectively. The initial linear temperature profile, $T(z) = (T_b - T_0)/h(x)$, where z is depth and x is horizontal position, means that even if the assumed initial basal temperature is $T_b = 1{,}300$ °C, there will be some thermal evolution in the model owing to both three-dimensional effects and assumed crustal heat production (Supplementary Fig. 3), which leads to a minor contribution to the total inferred rock uplift (Fig. 3b).

As temperatures equilibrate in the thermal boundary layer, the rock uplift calculated in the model is consistent with rapid rates of rock uplift immediately upon imposition of the basal perturbation, with higher uplift rates at the margins of the plateau than in the interior (Fig. 3d). Uplift rates decrease through time as the system approaches the steady state, and the final rock uplift is determined by both the final thermal structure and the assumed shape of the thermal boundary layer. In the steady state, the isotherms will be smoother than they were initially, but will mimic the shape of the thermal boundary layer (in the same manner that isotherms mimic topography near the surface). We assume that the transition from the thicker thermal boundary layer (200 km) beneath the plateau to the thinner thermal boundary layer (200 km – h; Fig. 3a) in the surrounding regions is given by the function atan(x/w), with a length scale of $w = d/10$ or $d/100$. The steady-state rock uplift roughly mirrors the shape of the protrusion in the thermal boundary layer, so although the rock uplift starts at a higher rate at the margins (Fig. 3b) and uplift rates slow down through time everywhere, the central region is predicted to continue uplifting longer than the margins. As a result, the point with maximum rock uplift at a given time migrates inward from the margin to the plateau interior (Fig. 3d).

31. Peterson, C. & Roy, M. in *Geology of the Chama Basin* (eds Brister, B. S., Bauer, P. W. & Read, A. S) 105–114 (56th Field Conf. Guidebook, New Mexico Geological Society, 2005).
32. Berman, S. C., Foland, K. A. & Spera, F. J. On the origin of an amphibole-rich vein in a peridotite inclusions from the Lunar Crater Volcanic Field, Nevada, U.S.A. *Earth Planet. Sci. Lett.* **56,** 343–361 (1981).
33. Condie, K. C., Cox, J., O'Reilly, S. Y., Griffin, W. L. & Kerrich, R. Distribution of high field strength and rare earth elements in mantle and lower crustal xenoliths from the Southwestern United States: the role of grain-boundary phases. *Geochim. Cosmochim. Acta* **68,** 3919–3942 (2004).
34. Ehrenberg, S. N. Petrogenesis of garnet lherzolite and megacrystalline nodules from the Thumb, Navajo Volcanic Field. *J. Petrol.* **23,** 507–547 (1982).
35. Feigenson, M. D. Continental alkali basalts of kimberlite and depleted mantle: evidence from Kilbourne Hole maar, New Mexico. *Geophys. Res. Lett.* **13,** 965–968 (1986).
36. Lauglin, A. W. & Brookins, D. G. Chemical and strontium isotopic investigations of ultramafic inclusions and basalt, Bandera Crater, New Mexico. *Geochim. Cosmochim. Acta* **35,** 107–113 (1971).
37. McGuire, A. V. & Mukasa, S. B. Magmatic modification of the uppermost mantle beneath the Basin and Range to Colorado Plateau Transition Zone; evidence from xenoliths, Wikieup, Arizona. *Contrib. Mineral. Petrol.* **128,** 52–65 (1997).
38. Roden, M. F., Irving, A. J. & Murthy, V. R. Isotopic and trace element composition of the upper mantle beneath a young continental rift: results from Kilbourne Hole, New Mexico. *Geochim. Cosmochim. Acta* **52,** 461–473 (1988).
39. Smith, D. & Riter, J. C. A. Genesis and evolution of low-Al orthopyroxene in spinel peridotite xenoliths, Grand Canyon field, Arizona, USA. *Contrib. Mineral. Petrol.* **127,** 391–404 (1997).
40. Wilshire, H. G. *et al.* Mafic and ultramafic xenoliths from volcanic rocks of the western United States. *Prof. Pap. US Geol. Surv.* **1443** (1988).
41. Baldridge, W. S. Mafic and ultramafic inclusion suites from the Rio Grande rift (New Mexico) and their bearing on the composition and thermal state of the lithosphere. *J. Volcanol. Geotherm. Res.* **6,** 319–351 (1979).
42. Beard, B. L. & Glazner, A. F. Trace element and Sr and Nd isotopic composition of mantle xenoliths from the Big Pine volcanic field, California. *J. Geophys. Res.* **100,** 4169–4181 (1985).
43. Bussod, G. Y. A. *Thermal and Kinematic History of Mantle Xenoliths from Kilbourne Hole, New Mexico.* Report No. LA-9616-T (Los Alamos National Laboratory, 1983).
44. Evans, S. H. Jr & Nash, W. P. Petrogenesis of xenolith-bearing basalts from southeastern Arizona. *Am. Mineral.* **64,** 249–267 (1979).
45. Fodor, R. V. Ultramafic and mafic inclusions and megacrysts in Pliocene basalt, Black Range, New Mexico. *Bull. Geol. Soc. Am.* **89,** 451–459 (1978).
46. Frey, F. A. & Prinz, M. Ultramafic inclusions from San Carlos, Arizona: petrologic and geochemical data bearing on their petrogenesis. *Earth Planet. Sci. Lett.* **38,** 129–176 (1978).
47. Galer, S. J. G. & O'Nions, R. K. Chemical and isotopic studies of ultramafic inclusions from the San Carlos Volcanic Field, Arizona: a bearing on their petrogenesis. *J. Petrol.* **30,** 1033–1064 (1989).
48. Hervig, R. L., Smith, J. V. & Dawson, J. B. Lherzolite xenoliths in kimberlites and basalts: petrogenetic and crystallochemical significance of some minor and trace elements in olivine, pyroxenes, garnet and spinel. *Trans. R. Soc. Edinb. Earth Sci.* **77,** 181–202 (1986).
49. Johnson, K. E. *An Appraisal of Mantle Metasomatism based upon Oxidation States, Trace Element and Isotope Geochemistry, and Fluid/Rock Ratios in Spinel Lherzolite Xenoliths.* PhD thesis, Northwestern Univ. (1990).
50. Riter, J. C. A. *Geochemical and Tectonic Evolution of the Colorado Plateau Mantle Lithosphere: Evidence from Grand Canyon Mantle Xenoliths.* PhD thesis, Univ. Texas, Austin (1999).
51. Rosenbaum, J. M., Zindler, A. & Rubenstone, J. L. Mantle fluids: evidence from fluid inclusions. *Geochim. Cosmochim. Acta* **60,** 3229–3252 (1996).
52. Smith, D. & Riter, J. C. A. Genesis and evolution of low-Al orthopyroxene in spinel peridotite xenoliths, Grand Canyon field, Arizona, USA. *Contrib. Mineral. Petrol.* **127,** 391–404 (1997).

53. Smith, D. & Levy, S. Petrology of Green Knobs diatreme, New Mexico, and implications for the mantle below the Colorado Plateau. *Earth Planet. Sci. Lett.* **19,** 107–125 (1976).
54. Roden, M. F. & Shimizu, N. Ion microprobe analyses bearing on the composition of the upper mantle beneath the Basin and Range and Colorado Plateau provinces. *J. Geophys. Res.* **98,** 14091–14108 (1993).
55. Tyner, G. N. & Smith, D. Peridotite xenoliths in silica-rich, potassic latite from the transition zone of the Colorado Plateau in north-central Arizona. *Contrib. Mineral. Petrol.* **94,** 63–71 (1986).
56. Wilshire, H. G., McGuire, A. V., Noller, J. S. & Turrin, B. D. Petrology of lower crustal and upper mantle xenoliths from the Cima Volcanic Field, California. *J. Petrol.* **32,** 169–200 (1991).

SUPPLEMENTARY INFORMATION

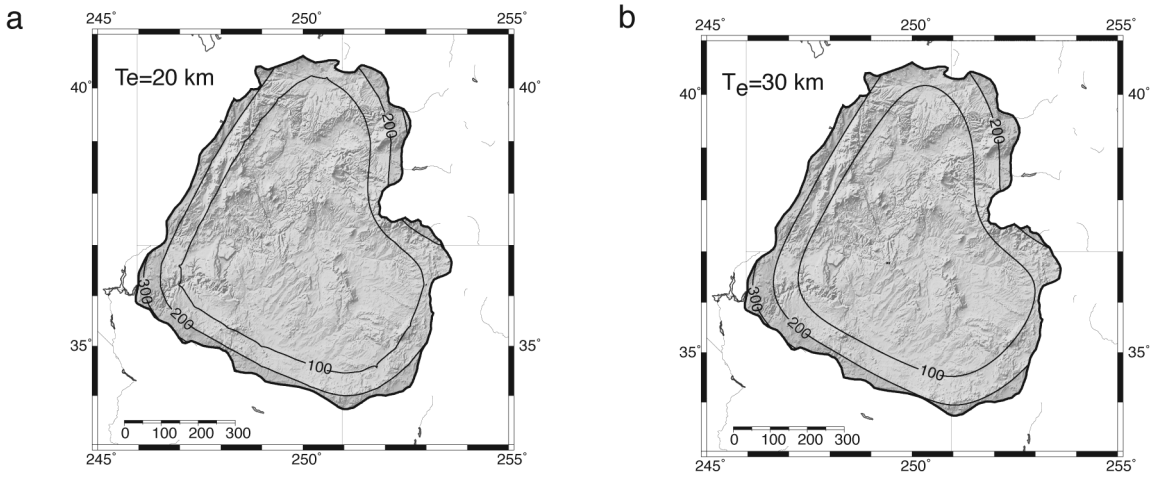

Supplementary Figure 1. Flexural response (in m) to extensional unloading adjacent to the CP. We assume a uniform upward load of 1.6×10^{12} N/m (equivalent to 700 m of erosion over a ~80 km-wide region) is present everywhere outside the CP and calculate the flexural response of a continuous, uniform-rigidity plate with effective elastic plate thickness Te of 20 km (a) and 30 km (b). Note that the flexural parameter in a is 46 km and in b is 63 km; this minor difference of 17 km in the flexural parameter does not greatly affect the flexural response of a region as large as the CP (diameter ~800 km).

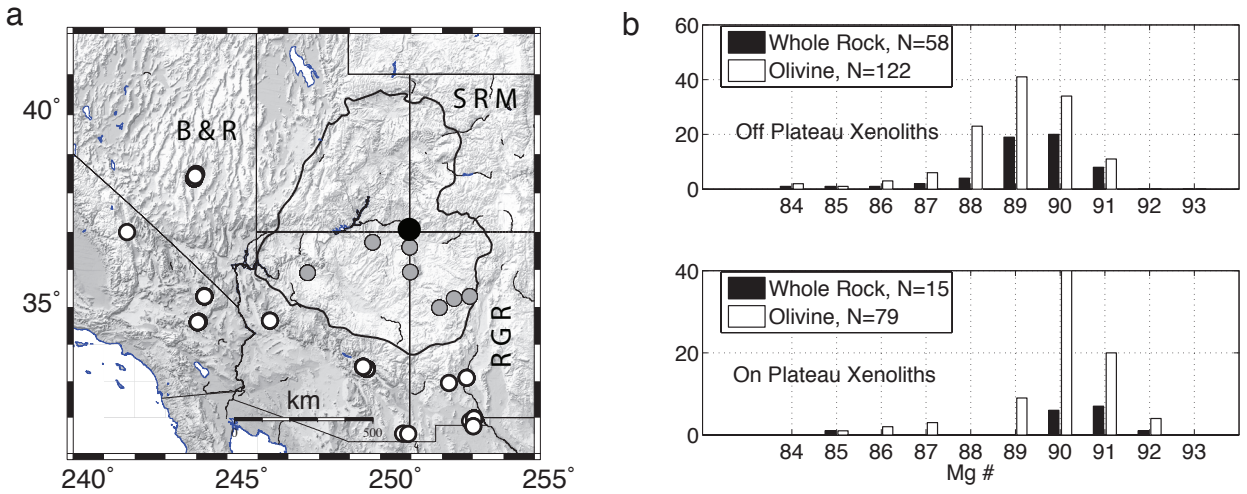

Supplementary Figure 2. Xenoliths and their compositions in the CP and surroundings. a Topography of the CP (outlined) and surrounding region (RGR=Rio Grande Rift; B&R=Basin and Range; SRM=Southern Rocky Mountains). Black dot marks the 'Four Corners' point and grey and white dots mark xenolith localities used in b. b Distribution of magnesium number for xenoliths on and off the plateau, constructed from published analysis (SI) and NAVDAT (North America Igneous Rock Database, http://geomaps.geo.ukans.edu/).

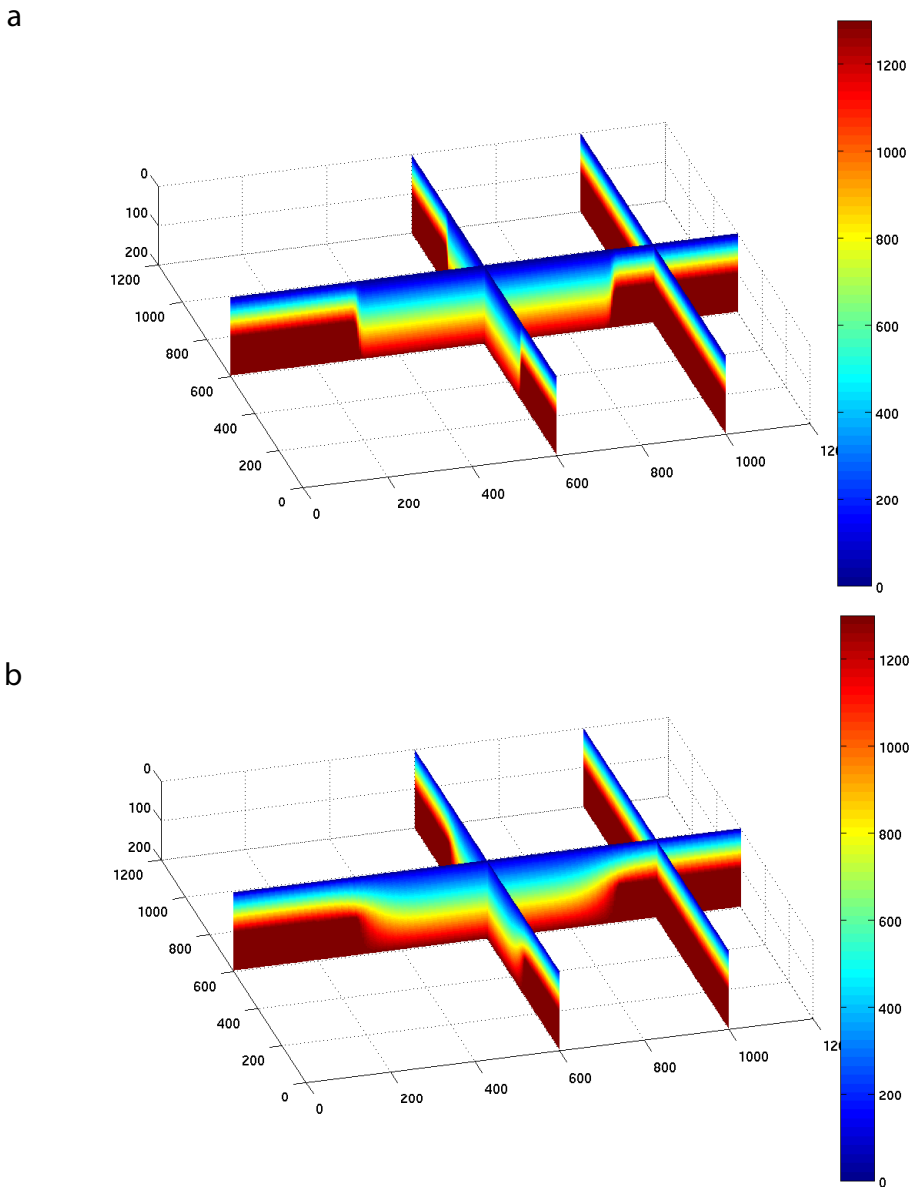

Supplementary Figure 3. Thermal structure evolution during conductive relaxation in a variable-thickness plate for $T_b = 1300\,^{o}C$. a Assumed initial thermal structure with linear geotherm at t=0 Myr. b Calculated thermal structure at t=50 Myr, after isotherms smoothen and the system approaches steady-state.